FRACTURE OF MATERIALS WITH STRAIN GRADIENT EFFECTS

Y. Huang*, L. Zhang, T. F. Guo, and K. C. Hwang
*Dept. of Mechanical Eng., Michigan Technological University, Houghton, MI 49931, USA
Dept. of Engineering Mechanics, Tsinghua University, Beijing 100084, China

ABSTRACT

Fracture in materials with *strain gradient effects* is studied by analytical and finite element methods, using Fleck and Hutchinson's strain gradient plasticity theory. Analytical solutions are obtained for the near-tip field in an elastic-plastic material with strain gradient effects. The mixed mode near-tip stress field in a power-law hardening solid is the *linear superposition* of its counterparts in mode I and II. The size of the dominance zone for the near-tip field is approximately l, the intrinsic material length on the order of a few microns. For an interface crack between dissimilar elastic-plastic materials with strain gradient effects, the analytical near-tip field does not agree with numerical results, indicating the existence of nonseparable fields.

KEYWORDS

Strain gradient effects, interface, crack-tip field, FEM.

INTRODUCTION

There are many experiments indicating that materials display strong size effect when the characteristic length associated with the deformation becomes small, typically on the order of microns. For example, the measured indentation hardness of metals and ceramics increases by a factor of two as the width of the indent is reduced from 10 microns to 1 micron (Nix, 1988; Stelmashenko et al., 1993; Ma and Clarke, 1995; Poole et al., 1996). As the wire diameter decreases from 170 to 12 microns, torsion of thin copper wires exhibits a systematic increase in torsion hardening (Fleck et al., 1994). Conventional plasticity theories based solely on strain hardening would not predict this size effect.

Fleck and Hutchinson (1993, 1996) and Fleck et al. (1994) developed the strain gradient plasticity based on the dislocation theory. Its fundamental is that the material hardening is due to statistically stored dislocations as well as geometrically necessary dislocations, and the latter is associated with plastic strain gradients (Nye, 1953; Cottrell, 1964; Ashby, 1970). A new length, l, considered as an intrinsic material length depending on microstructures, is introduced in strain gradient plasticity. When the representative length of the deformation field L is significantly larger than the intrinsic material length l, strain gradient effects become negligible and the theory degenerates to conventional plasticity. However, as L becomes comparable to or smaller than l, strain gradient effects come into play (Fleck and Hutchinson, 1996). The strain gradient plasticity can predict the size effect observed in experiments.

Due to stress singularity, large strain gradients exist near the tip of a crack in materials. The strain gradient effects become important when the crack tip process zone size is comparable to the intrinsic material length (Xia and Hutchinson, 1995; Fleck and Hutchinson, 1996), l, typically on the order of microns. The present paper provides an investigation of the strain gradient effects in fracture of homogeneous as well as bimaterial systems. It begins with a summary of strain gradient plasticity theory, while details can be found in Fleck and Hutchinson (1993, 1996) and Fleck et al. (1994).

SUMMARY OF STRAIN GRADIENT PLASTICITY THEORY

The generalized stresses are Cauchy stresses t_{ij} and couple stresses m_{ij}; the corresponding strain measures and displacements are strains ε_{ij}, displacements u_i, and curvatures χ_{ij}, rotations ω_i. The (unsymmetric) Cauchy stresses are decomposed to the symmetric part σ_{ij} and anti-symmetric part τ_{ij}. Equilibrium of forces and moments requires

$$t_{ji,j} = \sigma_{ji,j} + \tau_{ji,j} = 0 , \quad m_{ji,j} + e_{ikl} t_{kl} = 0 \tag{1}$$

where $\mathbf{e}$ is the permutation tensor. The kinematics analysis gives strains, rotations, and curvatures in terms of displacements,

$$\varepsilon_{ij} = (u_{i,j} + u_{j,i}) / 2 , \quad \omega_i = e_{ijk} u_{k,j} / 2 , \quad \chi_{ij} = \omega_{i,j} \tag{2}$$

The elimination of displacements and rotations yields the χ–ε compatibility equations and χ compatibility equations,

$$\chi_{ij} = e_{ikl} \varepsilon_{jl,k} , \quad e_{ikl} \chi_{jk,l} = 0 \tag{3}$$

The constitutive law for the deformation theory of strain gradient plasticity can be written as

$$\sigma_{ji} = \partial W / \partial \varepsilon_{ij} , \quad m_{ji} = \partial W / \partial \chi_{ij} \tag{4}$$

where the strain energy density W depends on the first invariant of strains $\varepsilon_m=\varepsilon_{kk}/3$ and second invariant of strains and curvatures, $\varepsilon_e=(6\varepsilon_{ij}\varepsilon_{ij}-2\varepsilon_{ii}\varepsilon_{jj})^{1/2}/3$, $\chi_e=(2\chi_{ij}\chi_{ij}/3)^{1/2}$, i.e.,

$$W = W (\varepsilon_e , l \chi_e , e_m) \tag{5}$$

The intrinsic material length l enters (5) from dimensional consideration. For an elastic solid with strain gradient effects, W takes the form (Koiter, 1964; Mindlin, 1964, 1965)

$$W = 3 G (\varepsilon_e^2 + l^2 \chi_e^2) / 2 + K \varepsilon_m^2 / 2 \tag{6}$$

where G and K are shear and bulk moduli, respectively. For an elastic-power law hardening solid with strain gradient effects, W is given by

$$W = n \Sigma_0 E_0 [(\varepsilon_e^2 + l^2 \chi_e^2) / E_0^2]^{(n+1)/(2n)} / (n + 1) + K \varepsilon_m^2 / 2 \tag{7}$$

where n(>1) is the plastic hardening power, Σ_0 and E_0 are reference stress and strain, such as uniaxial yield stress and strain related via Young's modulus E by $E_0=\Sigma_0/E$.

Each boundary has five independent boundary conditions in strain gradient theory. At a boundary with prescribed tractions, they are

$$n_j [t_{ji} - e_{ijk} (m_{pq} n_p n_q)_{,k} / 2] = T_i , \quad n_j m_{ji} - m_{pq} n_p n_q n_i = q_i \tag{8}$$

where $\mathbf{n}$ is the unit normal at the boundary, and T_i and q_i are reduced stress tractions and couple stress tractions. At a boundary with prescribed displacements, three components of displacements and two tangential components of rotations are given.

FRACTURE OF HOMOGENEOUS MATERIALS WITH STRAIN GRADIENT EFFECTS

Elastic Materials with Strain Gradient Effects

For an elastic material with strain gradient effects, Sternberg and Muki (1967) and Atkinson and Leppington (1977) investigated mode I fracture for a finite crack subjected to remote uniform tension and a semi-infinite crack with exponentially decayed symmetric traction on the crack surface. Huang et al. (1995) established that the mode I asymptotic near-tip field also has the square-root singularity, but is governed by two parameters, one for singular stresses and the other for singular couple stresses. The additional parameter comes from the irrotation of the deformation field near a crack tip. The dominant, singular stresses give a vanishing couple stress field, while the dominant, singular couple stress field comes from second order stresses.

The mode II near-tip field is also irrotational, but couple stresses are bounded, with only one parameter governing singular field in mode II (Huang et al., 1996). The mixed mode near-tip field has the structure in polar coordinates (r, θ)

$$\mathbf{t} = [B_I \mathbf{t}_I(\theta) + B_{II} \mathbf{t}_{II}(\theta)] r^{-1/2} , \quad \mathbf{m} = l A_I \mathbf{m}_I(\theta) r^{-1/2} \tag{9}$$

where subscripts I and II correspond to mode I and II, B and A are amplitudes of the near-tip stress and couple stress fields, respectively, and $\mathbf{t}_I(\theta)$, $\mathbf{t}_{II}(\theta)$ and $\mathbf{m}_I(\theta)$ are nondimensional angular functions given in Huang et al. (1996). For anti-plane deformation, the near-tip field has the structure (Zhang et al., 1996b)

$$\sigma = B_{III} r^{1/2} \sigma_{III}(\theta) / l , \quad \mathbf{m} = l B_{III} r^{-1/2} \mathbf{m}_{III}(\theta) , \quad \tau = l B_{III} r^{-3/2} \tau_{III}(\theta) \tag{10}$$

The symmetric stress is not singular around the crack tip, while the anti-symmetric has the $r^{-3/2}$ singularity but does not violate the requirement that the strain energy around the crack tip is finite. It is similar to Schiermeier and Hutchinson's (1996) mode III crack tip in strain gradient plasticity. The high-order singularity comes from the rotation in anti-plane deformation.

Zhang et al. (1996b) used the Wiener-Hopf method to investigate the transition from the classical K field ($r^{-1/2}$) to the new mode III near-tip field ($r^{-3/2}$) in (10). For an infinite elastic materials with strain gradient effects containing a semi-infinite crack, the classical K field was imposed as the remote boundary condition. It is established that the new asymptotic field dominates within a zone of $0.5l$ around the crack tip, while strain gradient effects are observed within $5l$. As the representative length associated with the deformation field becomes comparable to or smaller than the intrinsic material length l, the stress level around the crack tip is increased significantly. Zhang et al. (1996a) made similar observations in mode I and II deformation. They investigated the transition from classical K fields to the new near-tip fields in (9) by the Wiener-Hopf method as well as by the finite element method [using the element designed by Xia and Hutchinson (1995) to capture the strain gradient dependence]. As r increases, stresses do not transit monotonically between these two fields; stresses decrease from the new near-tip field to a level below the classical K field, and then gradually increase to approach the K field. The reasonable agreement between these two approaches provides another validation of the finite element method.

Elastic-Plastic Materials with Strain Gradient Effects

The path-independent J-integral (Rice, 1968) for materials with strain gradient effects is given by (Huang et al., 1995; Xia and Hutchinson 1995)

$$J = \int_\Gamma (W n_1 - T_i u_{i,1} - q_i \omega_{i,1}) ds \tag{11}$$

where Γ is an arbitrary contour surrounding the crack tip, originating and ending at lower and upper crack surfaces, respectively, W is the strain energy density, $\mathbf{n}$ is the unit normal on the contour, and $\mathbf{T}$, $\mathbf{u}$, $\mathbf{q}$, and ω are stress traction, displacement, couple stress traction, and rotation, respectively. For an elastic-power law hardening solid with the constitutive law in (4) and (7), Huang et al. (1995) and Xia and Hutchinson (1995) established that the near-tip asymptotic stress field has the same order of singularity as the HRR field (Hutchinson, 1968; Rice and

Rosengren, 1968). It is also controlled by a single parameter, J-integral, because couple stresses are less singular and are not the dominating terms near a crack tip,

$$\begin{Bmatrix} t_{rr} \\ t_{r\theta} \\ t_{\theta r} \\ t_{\theta\theta} \end{Bmatrix} = \frac{2n\Sigma_0}{\sqrt{3}(n+1)}\left[\frac{(n+1)J}{2\pi n\Sigma_0 E_0 r}\right]^{1/(n+1)} \begin{Bmatrix} \cos\frac{1}{n+1}\theta - \frac{1}{n}\cos\frac{n+2}{n+1}\theta \\ -\sin\frac{1}{n+1}\theta + \frac{1}{n}\sin\frac{n+2}{n+1}\theta \\ \sin\frac{1}{n+1}\theta + \sin\frac{n+2}{n+1}\theta \\ \cos\frac{1}{n+1}\theta + \cos\frac{n+2}{n+1}\theta \end{Bmatrix}$$

$$\mathbf{m} = o\left[r^{-1/(n+1)}\right] \tag{12}$$

where n, Σ_0, E_0 and J are the plastic hardening power, reference stress and strain, and J-integral, respectively. [Huang et al. (1995) established that there is another possible asymptotic field in which couple stresses dominate and stresses become less singular. This field, however, has not been verified by FEM.] The analytic solution in (12) is obtained because the near-tip field is irrotational as well as incompressible. For an elastic-perfectly plastic solid (n=∞) with strain gradient effects, stresses become $t_{rr}=2\Sigma_0/\sqrt{3}$, $t_{r\theta}=0$, $t_{\theta r}=2\Sigma_0\sin\theta/\sqrt{3}$, and $t_{\theta\theta}=2\Sigma_0(1+\cos\theta)/\sqrt{3}$, which are completely different to the Prandtl field in conventional materials.

The mode II near-tip field is obtained analytically by Xia and Hutchinson (1995). Stresses are the same as those in (12) except that cos and sin are replaced by -sin and cos, respectively. Huang et al. (1996) established that, for an elastic-power law hardening solid with strain gradient effects, the mixed mode near-tip stress field is the linear superposition of its counterparts in mode I and II. This linear superposition for nonlinear materials also results from irrotation and incompressibility in in-plane deformation for strain gradient materials. [Unlike mode I, it is impossible to have a couple stress-dominated field in mode II (Huang et al., 1996). The couple stress-dominated field under mixed mode loading is identical to that in mode I.]

Xia and Hutchinson (1995) presented a finite element study for mode I and II fracture in strain gradient plasticity. The HRR field was imposed as the remote boundary condition in the finite element study. Numerical results showed that the transition from the HRR field to the new near-tip field occurs smoothly. The HRR field is accurate for $r>5l$; the singular field becomes reasonably accurate for $r<l/5$; and a graduate transition region lies between, where r is the distance to the crack tip and l is the intrinsic material length. The HRR field was imposed at $r=10l$ to ensure the remote boundary condition is effectively applied.

Using the same element designed by Xia and Hutchinson (1995) to capture the strain gradient dependence, Zhang et al. (1996a) investigated mode I and II fracture under small scale yielding condition. The classical K field (i.e., the crack tip field in conventional materials without strain gradient effects) was applied as the remote boundary condition. Displacements from the classical K field was imposed at $r=10^4l$, the boundary of the finite element mesh. Only upper half plane was analyzed due to symmetry. There were 30 layers of elements in the circumferential direction, and 81 layers in the radial direction. The size of the smallest element near the crack tip is $10^{-3}l$, and effort is made to ensure elements having aspect ratios close to one. Numerical results for plastic hardening power n=10 and 3 are obtained, but only those for n=10 are presented in this paper. [A solid with a piecewise elastic/power law hardening stress-strain relation in uniaxial tension is used to better characterize the plastic yielding.]

Figure 1 shows the angular distribution of Σ for mode II stress intensity factor $K_{II}=20\Sigma_0 l^{1/2}$ and several r/l, where $\Sigma=(\sigma_e^2+m_e^2/l^2)^{1/2}$ is a combined measure of effective stress σ_e and effective couple stress $m_e=(3m_{ij}m_{ij}/2)^{1/2}$. The maximum plastic zone size is $260l$, only 2.6% of the overall finite element domain so that the small scale yielding condition is met. The near-tip asymptotic field corresponds to a horizontal line in Fig. 1 because Σ is independent of polar angle θ (Xia and Hutchinson, 1995; Huang et al., 1996). The mode II HRR field (Symington et al., 1988), which clearly exhibits a dependence on θ, is also shown in Fig. 1. The angular distributions for small r (e.g., $r/l=0.0041$, 0.024 and 0.21) agree well with the near-tip field; the distribution for $r=12.3l$ is very close to the HRR field; and the curve for $r=1.63l$ corresponds to a transition between two fields. For $K_{II}=20\Sigma_0 l^{1/2}$, finite element results agree reasonably well (within 10% differences) with the near-tip asymptotic field in a zone of size l around the crack tip. The zone of dominance for the near-tip field is larger than that observed in Xia and Hutchinson (1995).

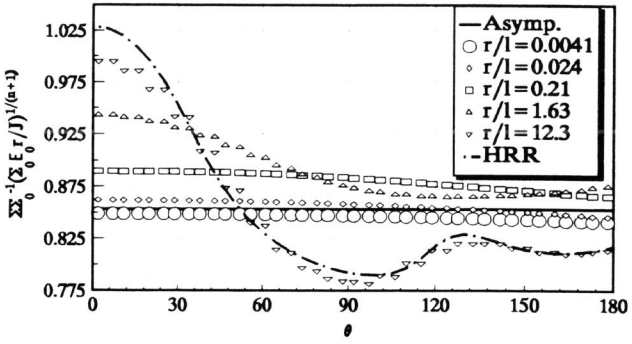

Fig. 1 Angular distribution of Σ for n=10, $K_{II}=20\Sigma_0 l^{1/2}$, and several r/l

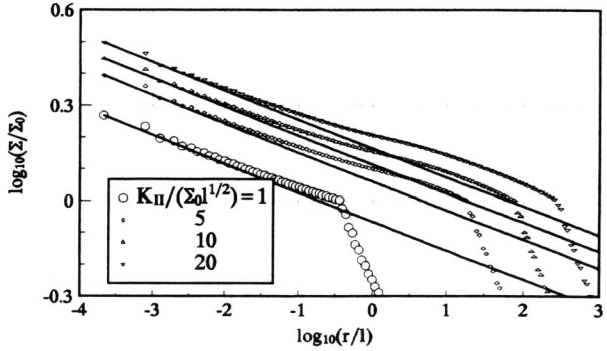

Fig. 2 Σ versus the distance r to crack tip in mode II for several $K_{II}/(\Sigma_0 l^{1/2})$; θ = 1.3 °

Figure 2 presents Σ/Σ_0 at polar angle θ = 1.3 ° versus the distance to crack tip, r/l, in logarithmic scales for four stress intensity factors. Each solid line represents a near-tip asymptote for the corresponding curve and the slope is the power of singularity, -1/(n+1). Finite element results agree well with the asymptotic field for small r. As r increases (hence strain gradient effects

become less significant), each curve eventually approaches a straight line with slope -1/2, corresponding to the classical K_{II} field. Transition between two fields exhibits very different characteristics for small and large loading. At a large stress intensity factor [e.g., $K_{II}/(\Sigma_0 l^{1/2})=10$ or 20], the curve contains another straight segment that is parallel to the initial straight line corresponding to the near-tip field. It has been verified that the angular distribution for any r in this straight segment agrees well with the HRR field (The segment is around $r=12.3l$, see Fig. 1). Therefore, the second straight segment on each curve corresponds to the HRR field. The classical K_{II} field transits to the HRR field, then to the new near-tip asymptotic field. However, the curve for a small stress intensity factor [e.g., $K_{II}/(\Sigma_0 l^{1/2})=1$] does not appear to have the second straight segment, so that stresses transit directly from the classical K_{II} field to the new near-tip field in the small plastic zone, not via the HRR field. Based on Figs. 1 and 2, it can be concluded that the size of dominance zone for the mode II near-tip asymptotic field is approximately l if $K_{II}>5\Sigma_0 l^{1/2}$, and is less than l (due to small plastic zone size) if $K_{II}<5\Sigma_0 l^{1/2}$.

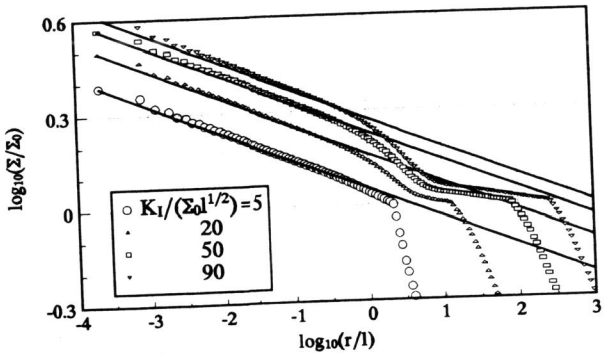

Fig. 3 Σ versus the distance to crack tip r in mode I for several $K_I/(\Sigma_0 l^{1/2})$; $\theta = 1.3°$

Figure 3 shows Σ/Σ_0 versus r/l at $\theta = 1.3°$ in mode I for stress intensity factor $K_I/(\Sigma_0 l^{1/2})=5$, 20, 50, 90. The maximum plastic zone size for $K_I/(\Sigma_0 l^{1/2})=90$ is $1060l$, more than 10% of the overall finite element domain ($r=10^4 l$). This barely meets the small scale yielding condition, so that $K_I/(\Sigma_0 l^{1/2})=90$ can be considered as the small scale yielding limit in the present finite element analysis. Similar to Fig. 2, each curve has a solid line as the near-tip asymptote [$\Sigma \sim r^{-1/(n+1)}$] for small r, and approaches the classical K_I field (the straight line with slope -1/2) for large r. However, as shown in Fig. 3 for $K_I \le 90\Sigma_0 l^{1/2}$, the second straight segment corresponding to the HRR field is either not observed or extremely small in mode I. Angular distributions of Σ for all r in the plastic zone do not show good agreement with the HRR field either. Therefore, under small scale yielding condition, stresses in mode I fracture transit from the classical K_I field to the near-tip asymptotic field via a large plastic zone, not via the HRR field. It is also observed that the size of dominance zone for the mode I near-tip field is approximately l if $K_I>5\Sigma_0 l^{1/2}$.

INTERFACE FRACTURE IN BIMATERIALS WITH STRAIN GRADIENT EFFECTS

The in-plane deformation for an interface crack between dissimilar materials with strain gradient effects is investigated. Solids above and below the interface are denoted by subscript 1 and 2.

Elastic Bimaterial Systems with Strain Gradient Effects

Governing equations for each constituent are the same as (1)-(6). The elastic shear modulus and Poisson's ratio are G_α and ν_α, and the intrinsic material length is l_α (α=1, 2) for each constituent. On the crack surfaces, boundary conditions in (8) become

$$t_{\theta\theta}(\theta=\pm\pi)=0, \quad t_{\theta r}(\theta=\pm\pi)=0, \quad m_{\theta 3}(\theta=\pm\pi)=0 \tag{13}$$

The continuity conditions at the interface (θ=0) are

$$[\,t_{\theta\theta}\,]=0, \quad [\,t_{\theta r}\,]=0, \quad [\,m_{\theta 3}\,]=0, \quad [\,u_r\,]=0, \quad [\,u_\theta\,]=0, \quad [\,\omega_3\,]=0 \tag{14}$$

where [ ] stands for the jump across the interface. The asymptotic field near an interface crack tip can be found similar to that for conventional bimaterials without strain gradient effects (e.g., Rice and Sih, 1965). It has the following structure in polar coordinates (r, θ)

$$\mathbf{t} = \mathrm{Re}\,[\,B\,\mathbf{t}_0(\theta)\,r^{-1/2+i\varepsilon}\,], \quad \mathbf{m} = l\,A\,\mathbf{m}_0(\theta)\,r^{-1/2} \tag{15}$$

where Re stands for the real part, B is the complex amplitude for stresses in the near-tip field, A is real amplitude for couple stresses, ε is the oscillatory index in plane strain given by

$$\varepsilon = \frac{1}{2\pi}\ln\left[\left(\frac{1}{G_1}+\frac{1-2\nu_2}{3-2\nu_2}\frac{1}{G_2}\right)\Big/\left(\frac{1}{G_2}+\frac{1-2\nu_1}{3-2\nu_1}\frac{1}{G_1}\right)\right] \tag{16}$$

(which is different to the oscillatory index in conventional bimaterials); the complex angular function $\mathbf{t}_0(\theta)$ and real angular function $\mathbf{m}_0(\theta)$ are given in the Appendix. The high-order asymptotic analysis shows that the dominant, singular couple stresses ($r^{-1/2}$) result from the second order stress field. Near the tip of an interface crack, stresses and couple stresses have the square-root singularity, but stresses are oscillatory and couple stresses are not. The near-tip amplitudes A and B depend on the applied loading, geometry of the component, and bimaterial properties such as moduli and intrinsic material lengths.

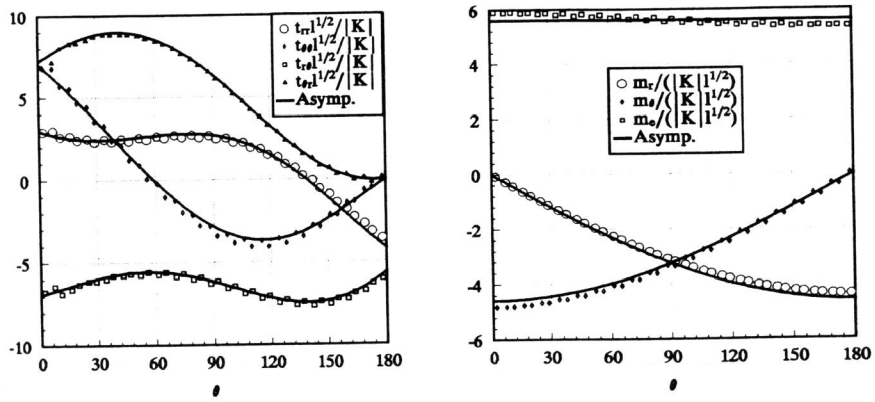

Fig. 4 Angular distributions of $\mathbf{t}$ and $\mathbf{m}$ for an interface crack with phase angle ψ=0; r=0.0039l

For an elastic material with strain gradient effects bonded to a rigid substrate ($G_2=\infty$), finite element method is used to investigate the transition from the classical, oscillatory K field for conventional bimaterials (e.g., Rice and Sih, 1965) to the new near-tip field in (15). The classical, oscillatory K field, characterized by its amplitude |K| and phase angle ψ (i.e., $K=|K|e^{i\psi}$), is imposed at the boundary of the finite element domain ($r=10^4 l$). Angular

distributions for stresses **t** and couple stress **m** are shown in Fig. 4 for K's phase angle $\psi=0$ and $r=0.0039l$, along with the asymptotic field in (15) in which near-tip amplitudes A and B are obtained by fitting the FEM results. The excellent agreement between numerical results and asymptotic field holds for all phase angles between 0 and 180°.

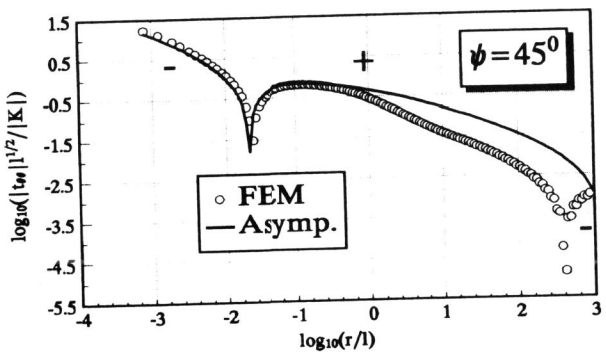

Fig. 5 $t_{\theta\theta}$ versus r for an interface crack with phase angle $\psi=45°$; $\theta=10.9°$

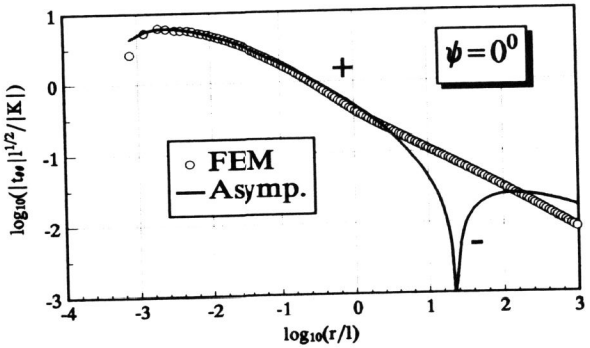

Fig. 6 $t_{\theta\theta}$ versus r for an interface crack with phase angle $\psi=0°$; $\theta=10.9°$

For K's phase angle $\psi=45°$, the stress component $t_{\theta\theta}$ at polar angle $\theta=10.9°$ is shown versus the distance r to crack tip in Fig. 5. The near-tip field is also shown in order to determine its zone of dominance. Due to oscillation, $t_{\theta\theta}$ can be positive or negative, as marked by + and - in Fig. 5. Finite element results agree well with the asymptotic field for small r, even on the location for $t_{\theta\theta}=0$ represented by the sharp spike in Fig. 5. Finite element analysis has captured the oscillatory nature of the field and has shown somewhat periodicity in oscillation with respect to $\log_{10}(r)$. No oscillation occurs for r between $10^{-1}l$ to $10^{2}l$ because the two spikes in Fig. 5 appear at small $r(<0.02l)$ and large $r(>400l)$. It is observed that the asymptotic field in (15)

dominates in a zone of l around the interface crack tip. The size of the dominance zone for the near-tip field decreases with the increase of K's phase angle ψ. For $\psi=0$, as shown in Fig. 6, the size of the dominance zone is more than $5l$, while the size is reduced to $0.5l$ for $\psi=90°$ (Fig. 7).

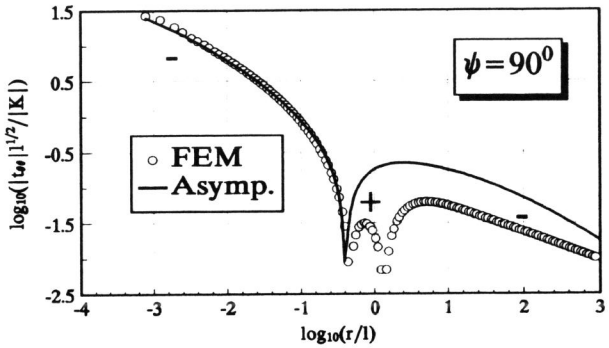

Fig. 7 $t_{\theta\theta}$ versus r for an interface crack with phase angle $\psi=90°$; $\theta=10.9°$

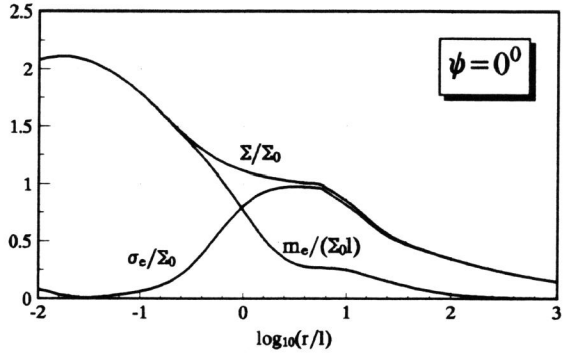

Fig. 8 σ_e, m_e, and Σ versus r for an interface crack with $|K|=10\Sigma_0 l^{1/2}$, $\psi=0$; $\theta=13.3°$

Elastic-Plastic Bimaterials with Strain Gradient Effects

The path-independent J-integral in (11) also holds for an interface crack between dissimilar elastic-plastic materials with strain gradient effects. The asymptotic field near an interface crack tip is investigated. Without loss of generality, the constituent above the interface has less plastic hardening, i.e., $n_1>n_2$. Similar to conventional bimaterials (e.g., Shih and Asaro, 1988, 1989), the near-tip field above the interface is identical to that for the same constituent bonded to a rigid substrate. Governing equations and crack surface boundary conditions are the same as (1)-(4), (7) and (13), while boundary conditions at the interface become

$$u_r=0\,,\quad u_\theta=0\,,\quad \omega_3=0 \tag{17}$$

Displacements in the near-tip field are assumed to have a separable, power-like form

$$\mathbf{u} = r^{p+1}\,\mathbf{u}_0(\theta) \tag{18}$$

where the power p and angular function $\mathbf{u}_0$ are to be determined. Strains, rotations, and curvatures are obtained from kinematics equation (2), while the constitutive law (4) and (7) give stresses and couple stresses in terms of r and $\mathbf{u}_0$. Equilibrium equation (1) leads to two homogeneous nonlinear ordinary differential equations for $u_{r0}(\theta)$ and $u_{\theta 0}(\theta)$, with homogeneous boundary conditions in (13) and (17). In order to have a non-trivial solution, the power p must be the eigenvalue and $\mathbf{u}_0$ be the eigenfunction. It gives the following near-tip asymptotic field

$$\begin{Bmatrix} m_{r3} \\ m_{\theta 3} \end{Bmatrix} = \sqrt{\frac{2}{3}}\Sigma_0 \left[\frac{J}{2I(n)\Sigma_0 E_0 r}\right]^{1/(n+1)} \left[\frac{n^2+1}{2n^2} + \frac{n^2-1}{2n^2}\cos 2[\theta-\varphi(\theta)]\right]^{1/(2n+2)} \begin{Bmatrix} \sin\varphi(\theta) \\ \cos\varphi(\theta) \end{Bmatrix}$$

$$\mathbf{t} = o\left[r^{-1/(n+1)}\right] \tag{19}$$

where $n=n_1$ is the power of hardening for the upper constituent, and

$$\varphi(\theta) = \frac{1}{2}\left[\theta - \sin^{-1}\left(\frac{n-1}{n+1}\theta\right)\right] \tag{20}$$

$$I(n) = \int_0^{\pi}\left\{\frac{n^2+1}{2n^2} + \frac{n^2-1}{2n^2}\cos 2[\theta-\varphi(\theta)]\right\}^{1/2}\left\{\frac{n}{n+1}\cos\theta + \sin[\theta-\varphi(\theta)]\sin[\varphi(\theta)]\right\}d\theta \tag{21}$$

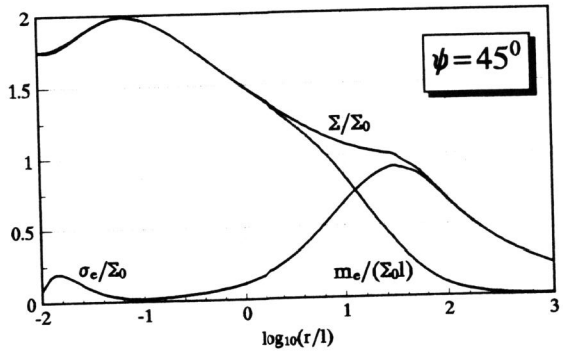

Fig. 9 σ_e, m_e, and Σ versus r for an interface crack with $|K|=10\Sigma_0 l^{1/2}$, $\psi=45°$; $\theta=13.3°$

It is observed that couple stresses have replaced stresses to become the dominating singular terms near an interface crack tip. They are not oscillatory, and have the $r^{-1/(n+1)}$ singularity. This is similar to conventional bimaterials without strain gradient effects where stress oscillation is rather weak or vanishes (Shih and Asaro, 1988, 1989). However, unlike the near-tip field in conventional bimaterials (Rice, 1988; Shih and Asaro, 1988, 1989), the new near-tip field is governed by the J-integral only, i.e. independent of K's phase angle ψ. Moreover, it has been verified that new near-tip field in (19) is identical to Huang et al.'s (1996) couple stress-dominated field in a homogeneous elastic-plastic solid (no interface) under mixed mode loading. The couple stress-dominated field in (19) results from the assumption that the near-tip field is separable and power-like as in (18). This type of solution does not exist and the numerically calculated near-tip fields are not separable and power-like for an interface crack between conventional bimaterials (Shih and Asaro, 1988, 1989). For bimaterials with strain gradient

effects, finite element results in the present study confirm that stresses and couple stresses are different to (19) near an interface crack tip. Figures 8, 9, and 10 present the effective stress σ_e, effective couple stress m_e, and $\Sigma=(\sigma_e^2+m_e^2/l^2)^{1/2}$ at polar angle $\theta=13.3°$ versus the distance to crack tip, r/l, for three phase angles of K, $\psi=0$, 45°, and 90°, and hardening power n=10, stress intensity factor $|K|=10\Sigma_0 l^{1/2}$. Couple stress m_e approaches zero at large $r(>100l)$ for all phase angles because of the remote classical K field. At small $r(<0.1l)$, however, couple stress (m_e/l) for phase angle $\psi=0$ and 45° (Figs. 8 and 9) is significantly larger than the effective stress σ_e, hence dominates the contribution to Σ. Although this seems to agree with the dominance of couple stresses in the near-tip field in (19), they are not the same. Couple stress in (19) decreases monotonically with respect to r, while Figs. 8 and 9 do not exhibit this feature for small r around $0.01l$. For phase angle $\psi=90°$, stresses as well as couple stresses are oscillatory so that the near-tip field is completely different to that in (19).

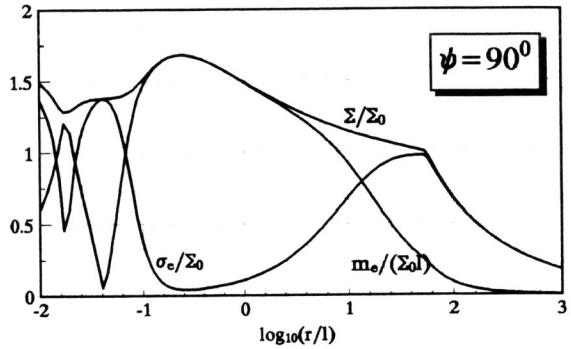

Fig. 10 σ_e, m_e, and Σ versus r for an interface crack with $|K|=10\Sigma_0 l^{1/2}$, $\psi=90°$; $\theta=13.3°$

ACKNOWLEDGMENTS

The authors acknowledge helpful discussions with J. W. Hutchinson, G. Ravichandran, C. F. Shih, W. Yang, and the support from the US National Science Foundation, ALCOA Foundation, and National Natural Science Foundation of China.

REFERENCES

Ashby, M. F. (1970). *Phil. Mag.*, **21**, 399-424.
Atkinson, C. and F. G. Leppington (1977). *Int. J. Solids Struct.*, **13**, 1103-1122.
Cottrell, A. H. (1964). *The mechanical properties of materials*. J. Willey.
Fleck, N. A. and J. W. Hutchinson (1993). *J. Mech. Phys. Solids*, **41**, 1825-1857.
Fleck, N. A. and J. W. Hutchinson (1996). Strain gradient plasticity. *Advances in Applied Mechanics* (eds. Hutchinson, J. W. & Wu, T. Y.) **33** (in press). Academic Press.
Fleck, N. A., G. M. Muller, M. F. Ashby and J. W. Hutchinson (1994). *Acta Metall. et. Mater.*, **42**, 475-487.

Huang, Y., L. Zhang, T. F. Guo and K. C. Hwang (1995). Near-tip fields for cracks in materials with strain gradient effects. In: *Proc. of the IUTAM Symposium on Nonlinear Fracture Mechanics* (ed. Willis, J. R.), Cambridge University, September 3-7, 1995.
Huang, Y., L. Zhang, T. F. Guo and K. C. Hwang (1996). Mixed mode near-tip fields for cracks in materials with strain gradient effects. *J. Mech. Phys. Solids* (in press).
Hutchinson, J. W. (1968). *J. Mech. Phys. Solids*, **16**, 13-31.
Koiter, W. T. (1964). *Proc. Ned. Akad. Wet. (B)*, **67**, 17-44.
Ma, Q. and D. R. Clark (1996). *J. Mater. Res.*, **10**, 853-863.
Mindlin, R. D. (1964). *Arch. Rational Mech Anal.*, **16**, 51-78.
Mindlin, R. D. (1965). *Int. J. Solids Struct.*, **1**, 417-438.
Nix, W. D. (1988). *Met. Trans. A*, **20A**, 2217-2245.
Nye, J. F. (1953). *Acta Metall.*, **1**, 153-162.
Poole, W. J., M. F. Ashby and N. A. Fleck (1996). *Scripta Metall. et. Mater.*, **34**, 559-564.
Rice, J. R. (1988). *J. Appl. Mech.*, **55**, 98-103.
Rice, J. R. & Rosengren, G. F. (1968). *J. Mech. Phys. Solids*, **16**, 1-12.
Rice, J. R. and G. C. Sih (1965). *J. Appl. Mech.*, **32**, 418-423.
Schiermeier, A. D. and J. W. Hutchinson (1996). Crack tip fields in an elastic-plastic strain gradient solid in mode III. to be published.
Shih, C. F. and R. J. Asaro (1988). *J. Appl. Mech.*, **55**, 299-316.
Shih, C. F. and R. J. Asaro (1989). *J. Appl. Mech.*, **56**, 763-779.
Stelmashenko, N. A., A. G. Walls, L. M. Brown and Y. V. Milman (1993). *Acta Metall. et. Mater.*, **41**, 2855-2865.
Sternberg, E. and R. Muki (1967). *Int. J. Solids Struct.*, **3**, 69-95.
Symington, M., C. F. Shih and M. Ortiz (1988). Tables of plane strain mixed-mode plastic crack tip fields. Division of Engineering, Brown University, Providence.
Xia, Z. C. and J. W. Hutchinson (1995). Crack tip fields in strain gradient plasticity. *J. Mech. Phys. Solids* (in press).
Zhang, L., T. F. Guo, J. Y. Chen, Y. Huang and K. C. Hwang (1996a). Analytic and finite element studies of mode I and II fracture in elastic/plastic materials with strain gradient effects (submitted for publication).
Zhang, L., Y. Huang, K. C. Hwang and J. Y. Chen (1996b). The mode III full field solution in elastic materials with strain gradient effects (submitted for publication).

APPENDIX

For simplicity, only $\mathbf{t}_0$ and $\mathbf{m}_0$ in the upper half plane ($0<\theta<\pi$) is presented. They are given by

$$\begin{Bmatrix} t_{rr0} \\ t_{r\theta 0} \\ t_{\theta r0} \\ t_{\theta\theta 0} \end{Bmatrix} = \begin{bmatrix} (1+\alpha)b_1 & (1+\alpha)b_2 & -c_1 & c_2 \\ (\alpha-\gamma_1)b_2 & -(\alpha-\gamma_1)b_1 & c_2 & c_1 \\ (\alpha+\gamma_1)b_2 & -(\alpha+\gamma_1)b_1 & c_2 & c_1 \\ (1-\alpha)b_1 & (1-\alpha)b_2 & c_1 & -c_2 \end{bmatrix} \begin{Bmatrix} \cos p\theta \\ \sin p\theta \\ \cos(p+2)\theta \\ \sin(p+2)\theta \end{Bmatrix}$$

$$m_{r0} = \sin(\theta/2),\ m_{\theta 0} = \cos(\theta/2) \tag{22}$$

where $p=-1/2+i\varepsilon$ is the power of stress singularity, and ε is given in (16); $\alpha=(1/2-\nu_1)p$; $\gamma_1=2(1-\nu_1)$; and b_1, b_2, c_1, and c_2 are given by

$$\begin{aligned} b_1 &= \gamma_2 + 1 + (\gamma_2 - 1)\mu, \quad b2 = (t - \gamma_1/t)\rho - (t + \gamma_2/t)\mu \\ c_1 &= (\gamma_2 + 1)(\alpha + \gamma_1 - 1) + [1 + (\gamma_2 - 1)\alpha + \gamma_1\gamma_2)]\mu \\ c_2 &= [(1-\alpha)t + \gamma_1(\alpha+\gamma_1)/t]\rho - [(1-\alpha)t - \gamma_2(\alpha+\gamma_1)/t]\mu \end{aligned} \tag{23}$$

where $\gamma_2=2(1-\nu_2)$; $\rho=(\gamma_2+1)/(\gamma_1+1)$; $\mu=G_1/G_2$ is the ratio of shear moduli; and $t=\tan(p\pi)$.